NACA

RESEARCH MEMORANDUM

INVESTIGATION OF INTERACTION EFFECTS ARISING FROM

SIDE-WALL BOUNDARY LAYERS IN SUPERSONIC

WIND-TUNNEL TESTS OF AIRFOILS

By

K. R. Czarnecki and C. F. Schueller

Langley Aeronautical Laboratory
Langley Field, Va.

NATIONAL ADVISORY COMMITTEE
FOR AERONAUTICS

WASHINGTON

November 3, 1948

NATIONAL ADVISORY COMMITTEE FOR AERONAUTICS

RESEARCH MEMORANDUM

INVESTIGATION OF INTERACTION EFFECTS ARISING FROM

SIDE-WALL BOUNDARY LAYERS IN SUPERSONIC

WIND-TUNNEL TESTS OF AIRFOILS

By K. R. Czarnecki and C. F. Schueller

SUMMARY

An investigation has been made to determine the cause for a discrepancy between theoretical and experimental pressure distributions found during a two-dimensional investigation of flapped airfoils in a 2- by 8-inch supersonic tunnel. The results of the investigation indicated a tunnel-boundary-layer and model-flow interaction effect on the flow over models mounted directly from the walls in supersonic wind tunnels. The interaction effects or disturbances were found to extend a considerable distance from the tunnel wall, particularly on surfaces where the Mach number approached unity. In general, strong disturbances propagated from the boundary layer in the wing-tunnel-wall juncture along a wave inclined at an angle slightly greater than the Mach angle for the local stream. An observation indicates that similar disturbances may arise from wing-fuselage junctures on supersonic airplanes.

INTRODUCTION

During an investigation of the aerodynamic characteristics of a two-dimensional flapped airfoil in a 2- by 8-inch supersonic tunnel a large discrepancy between theoretical and experimental pressure distributions was found. In order to determine the cause for this disagreement, total- and static-pressure surveys were made in the test nozzle in the vicinity of the model location both with the model installed and with the jet empty.

SYMBOLS

c   chord of model

c_p specific heat at constant pressure

c_v specific heat at constant volume

H   total or stagnation pressure

M   Mach number

p   static pressure

P   pressure coefficient $\left(\dfrac{p - p_0}{q_0} \right)$

q   dynamic pressure $\left(\dfrac{1}{2}\rho V^2 \right)$

R   Reynolds number $\left(\dfrac{\rho_0 V_0 c}{\mu} \right)$

μ viscosity

V   velocity

α angle of attack of airfoil, degrees

γ ratio of specific heats $\left(\dfrac{C_p}{C_v} = 1.4 \right)$

δ angle of flap chord with respect to airfoil chord (trailing
             edge down, positive), degrees

ρ mass density of air

Subscripts:

o   free stream

T   uncorrected total pressure measured by a total-pressure probe

The absence of a subscript denotes local conditions.

APPARATUS AND METHODS

Wind tunnels.— A 2— by 8—inch supersonic tunnel in which the tests
were made is a closed—return type powered by two centrifugal blowers. The
moisture content of the tunnel air stream can be controlled over a moderate
range by bleeding dry air into the tunnel system ahead of the blowers and
bleeding air out just ahead of the tunnel entrance section. During a test
the amount of dry air bled in and mixed air bled out was adjusted to obtain
the desired moisture content in the air stream. All data presented in this
paper were obtained with the quantity of the water vapor in the tunnel
air stream kept to values sufficiently low so that the effects of
condensation in the supersonic nozzle were negligible. The Mach number
in the test section was about 1.68.

All models used in the investigation were supported directly from the walls and were sealed at the airfoil-wall juncture to prevent end leakage. When an airfoil is tested at high angles of attack, a Mach reflection occurs between the high-pressure side of the airfoil and the tunnel wall which may cause the reflected bow wave to impinge on the model. In order to extend the range of angles of attack free from such interference effects, the models were located $1\frac{1}{2}$ inches above the nozzle axis and tests were generally made only at positive angles of attack. In addition, the upper and lower surfaces of the tunnel were given a small amount of relief at a point approximately opposite the midchord point of the model.

Test models.— The test models were of solid brass, completely spanned the test section, and had 2-inch chords. Models having a symmetrical 10-percent-thick circular-arc airfoil section with a 40-percent-chord flap and with a 20-percent-chord flap were investigated. The models are believed to be accurate within plus or minus 0.003 inch, and the gap between the flap leading edge and the fixed portion of the airfoil was 0.003 inch or 0.0015 chord. This gap was not sealed during the tests.

Two models were required for each flap configuration because pressure tubes could not be brought out of the necessarily small trunnions of the schlieren models. Figure 1 presents a schematic layout of the geometric characteristics and figure 2 presents the location of the 0.020-inch-diameter pressure orifices of the 0.20c flapped model. The construction and tube installation of the 0.40c flapped model were similar. The location of the models in the nozzle and, in particular, their relation to the location of the schlieren is indicated in figure 3. Figure 4 is a photograph of the 0.40c pressure-distribution model.

Based on a chord of 2 inches, the Reynolds number for the tests was about 750,000.

Pressure measurements.— The test-section wall pressures and pressures on the models were recorded simultaneously by photographing a multitube mercury manometer. All other pressures were read visually. The spanwise total-pressure surveys were made with probes having a 0.050-inch outside diameter and square heads; the static-pressure surveys were made with probes having a 0.040-inch outside diameter with four orifices at 90° spacing located five diameters back from a spherical head. Across the large tunnel width, the total-pressure surveys were made with a $\frac{1}{8}$-inch outside diameter probe having a rounded head. All probes were alined with the tunnel center line; hence, aft of the bow wave from the model leading edge the probes were no longer parallel to the local stream. In the case of the total-pressure probe, the effect of the misalinement on the accuracy of the readings is believed to be small inasmuch as all

total-pressure surveys made with the model installed were made with the
square-end total-pressure probes. Most of the spanwise-pressure surveys
were made in two planes: a plane parallel to and 1/2 inch below the
center line of the airfoil at $\alpha = 0^{\circ}$ and a plane perpendicular to the
free-stream flow and passing through the leading edge of the model.
Locations of the actual survey stations are given in figure 5. In order
to insure that any disturbance from the airfoil-flap juncture would be
as far back on the airfoil as possible, the 0.20c flapped model was
installed for this series of tests.

The theoretical pressure distributions for the circular-arc sections
are based on the pressure rise relationships determined from oblique
shock theory and Meyer's equations for the expansion of a two-dimensional
supersonic flow and were obtained by using the tables presented in
reference 1.

Schlieren system.— The schlieren equipment for the 2— by 8-inch
supersonic tunnel consisted of two 39-inch focal length parabolic front-
surface mirrors with a spark-gap light source having a duration of
approximately 6 microseconds. The schlieren windows in the tunnel were

ordinary $\frac{1}{2}$-inch plate glass.

<div align="center">RESULTS AND DISCUSSION</div>

During an investigation of the aerodynamic characteristics of a
two-dimensional flapped airfoil in a 2— by 8-inch supersonic tunnel, a
large discrepancy between theoretical and experimental pressure
distributions was found. An example of the discrepancy, which at its
maximum amounted to over $0.10q_{o}$ between the 30- and 40-percent-chord
stations, is shown in figure 6. It may be noted that as the angle of
attack is increased the discrepancy on the lower or high-pressure surface
increased numerically and tended to spread while that on the upper or
low-pressure surface showed no great change except for a possible
movement rearward. The disagreement occurred, as the data in the figure
show, in tests of two different models and thus eliminated the possibility
that excessive random variations in model contour or any appreciable
pressure-orifice error were to blame. Further, calculations based upon
the measured deviations in model contours from the true circular-arc
sections indicated that only minor variations in pressure distributions
should be expected. The comparison between theoretical and experimental
pressure distributions is not extended to angles of attack beyond 2°,
inasmuch as the shock theoretically detaches itself from the nose of
the airfoil at higher values of α investigated and results in a
local region of subsonic flow at the leading edge of the airfoil.
When this occurs, the theory used to calculate the pressure distributions
is no longer valid.

Schlieren photographs of the models at α and $\delta = 0^\circ$, corresponding to the data presented for the lower angles of attack in figure 6, are shown in figure 7. Except for indicating that the leading-edge shock may be detached for at least part of the airfoil span, the photographs do not show any irregularities originating from the top or bottom of the nozzle which could account for the irregularity of the measured pressure distributions. The indication that the bow wave is detached over part of the airfoil span is not surprising when it is considered that more than a fourth of the model is immersed in the tunnel-wall boundary layer where the Mach number is sufficiently low for detachment to occur.

The test nozzle was then surveyed, with models removed, in the 2-inch or spanwise direction by means of total- and static-pressure tube probes and in the 8-inch direction by a total-head tube probe, and the results of the total-pressure surveys plotted as the non-dimensional pressure ratios H_T/H_0 are shown in figures 8 and 9. No static-pressure surveys are shown because it was found that interference effects set up by the bow wave from the head of the static probe precluded satisfactory measurements near the tunnel boundary layer. The total pressure H_0, which is identical to the stagnation pressure, was determined from the subsonic flow just ahead of the supersonic nozzle and a tunnel calibration against humidity effects. It may be seen that outside the boundary layer, which is approximately 0.30 inch thick, the variation in the pressure ratios across the nozzle was small, which indicated that reasonably uniform flow was attained. The direction of the flow in the nozzle also appears to be very nearly parallel to the tunnel center line since practically zero lift was obtained on the pressure-distribution models at $\alpha = 0^\circ$ and $\delta = 0^\circ$, and these angles were set by alining the model with the tunnel center line.

It was suspected that the discrepancy in pressures might be caused either by boundary-layer transition on the model or by disturbances arising from the side walls of the nozzle as a result of shock-tunnel-boundary-layer interaction near the leading edge of the model when the model is installed. It is possible that neither one of these disturbances would appear on the schlieren photographs. The first possibility was quickly eliminated when no change in the experimental pressure distribution occurred over the forward portion of the airfoil where the discrepancy was centered with transition fixed near the leading edge by means of a strip of carborundum grains. The second possibility was first investigated by measuring the wall static pressures along the axis of the tunnel for a distance of more than 1 model chord length ahead of the leading edge. The results, shown on figure 10 for $\alpha = 0^\circ$, do not indicate the presence of any disturbance from the tunnel wall in the range of angles of attack investigated (from 0° to 4°) at least to within 1/4 inch of the model leading edge. Spanwise total- and static-pressure surveys were then made in the vicinity of the model for a range of model angles of attack and these indicate the presence of a disturbance. Some typical results from the total-pressure surveys are presented in figures 11 and 12. No static-pressure-distribution data are presented because it was found that

in most surveys the static probe crossed a shock and the pressures behind
the shock were transmitted forward through the subsonic boundary layer
on the probe, thus making it impossible to obtain satisfactory static-
pressure data. It was not readily feasible to overcome this difficulty
on the present setup. The static-pressure surveys, however, do corrobo-
rate the fact that some kind of disturbance is present. Some interference
no doubt also was caused by the introduction of the total-pressure probe
into the stream near the origin of the disturbances being investigated,
but its magnitude appeared small and the results of the total-pressure
surveys should be nearly correct.

Figure 11, which is a plot of some of the spanwise-total-pressure
surveys in the plane parallel to and 1/2 inch below the model center line,
indicates that as the model is approached from the upstream direction
a "hump" appears in the measured total pressures (plotted here as the
nondimensional pressure ratio H_T/H_o) near the outer edge of the tunnel
boundary layer. This hump or increase in measured total pressure spreads
toward the center of the tunnel on the surveys made further downstream
and finally merges with the disturbance from the other side of the tunnel.
Beyond the point where the disturbances have merged, a second hump, less
clearly defined, appears in the center of the tunnel as exemplified by
the curve for the station 1.20 inches aft of the leading edge of the model.
The pressures of the initial hump have dropped off probably because this
survey station was behind the bow wave from the model leading edge where
the stagnation pressure is lower and the local Mach number is higher than
that in the free stream. Figure 12 shows that the same general trend
occurred at a station at the leading edge and 1 inch below the model
center line when α was increased.

A trace of the inner edge of the disturbance in the plane 1/2 inch
below the model center line is shown in figure 13. It was necessary
to average the values from both sides of the tunnel and for two values
of α to obtain a smooth curve, particularly after the disturbances
from both sides of the tunnel merged; therefore, caution must be used
in interpreting the curve. The curve appears to indicate, however, that
the disturbance must be associated with a compression or shock inasmuch
as the curve in the region ahead of the bow wave from the airfoil is
inclined at an angle greater than the Mach angle for the free stream.
A plot of the tunnel-boundary-layer thickness is included, although in
the region where the disturbance originates it is impossible to
differentiate accurately between boundary layer and disturbance and this
difficulty may account, at least partly, for the apparent thickening of
the boundary layer at this point. Analysis of all the total-pressure
surveys reveals that the disturbance usually originates between 1/2
and 3/4 inch ahead of the leading-edge-shock locations indicated by
the corresponding schlieren photographs. It is possible that the
introduction of the probe into the disturbance may have caused it to
move forward slightly, but probably not to this extent. The location of
the initial appearance of the disturbances as determined from the total-
pressure surveys does not agree with the indication of the tunnel-wall

static pressures of figure 10. The reason for the disagreement is not known, but may be associated with the small number and relatively large spacing of the wall stations near the leading edge of the airfoil.

The fact that the hump in the total-pressure surveys must be associated with a compression can be shown analytically. By Rayleigh's formula, or the supersonic pitot-tube equation, it is known that

$$\frac{H_T}{p} = \frac{\gamma + 1}{2} M^2 \left[\frac{(\gamma + 1)^2 M^2}{4\gamma M^2 - 2(\gamma - 1)} \right]^{\frac{1}{\gamma - 1}} \tag{1}$$

in the supersonic part of the stream, where H_T is the total pressure read by a probe and p and M are the static pressure and Mach number, respectively, at the point. In order to derive the equation, it is assumed that the stream is decelerated to a subsonic Mach number through a normal shock ahead of the tube and thence compressed adiabatically from the Mach number behind the shock to stagnation pressure at $M = 0$. It is this stagnation pressure which is registered on the manometer. In the subsonic part of the stream, where no shock forms ahead of the tube, the corresponding relation is

$$\frac{H_T}{p} = \left(1 + \frac{\gamma - 1}{2} M^2 \right)^{\frac{\gamma}{\gamma - 1}} \tag{2}$$

It should be noted that equation (2) is essentially the equation for the stagnation-pressure ratio in either subsonic or supersonic flow and that H_T becomes equal to the stagnation pressure in subsonic flow. The ratio of the measured total-pressure to the free-stream stagnation pressure is then given by

$$\frac{H_T}{H_0} = \frac{p}{p_0} \frac{\frac{\gamma + 1}{2} M^2 \left[\frac{(\gamma + 1)^2 M^2}{4\gamma M^2 - 2(\gamma - 1)} \right]^{\frac{1}{\gamma - 1}}}{\left(1 + \frac{\gamma - 1}{2} M_0^2 \right)^{\frac{\gamma}{\gamma - 1}}} \tag{3}$$

for supersonic flow and

$$\frac{H_T}{H_O} = \frac{p}{p_O} \frac{\left(1 + \frac{\gamma - 1}{2} M^2\right)^{\frac{\gamma}{\gamma-1}}}{\left(1 + \frac{\gamma - 1}{2} M_O{}^2\right)^{\frac{\gamma}{\gamma-1}}} \tag{4}$$

for subsonic flow, where the absence of a subscript denotes conditions locally at a point and the subscript o denotes average conditions in the free stream.

A plot of H_T/H_O as a function of the Mach number ratio M/M_O over the range from 0 to 1 is given in figure 14 with p assumed constant and equal to p_O, as p will be in a well-designed nozzle with no disturbances present. The figure indicates that no hump in the curves is possible either in a boundary layer where the Mach number increases continuously from the tunnel wall to the free stream or in the free stream if the flow is uniform. It then becomes obvious that, in order to obtain the hump in the measured-total-pressure curves, a local region of increased static pressure must exist or the pressure must be measured behind an oblique shock or multiple shocks, whence equations (1) and (3) are no longer valid. In either case a disturbance involving a compressive process is indicated.

The fact that a compressive disturbance originates near the leading edge of the airfoil can explain qualitatively the type of pressure distributions obtained in the airfoil tests in the 2- by 8-inch tunnel (fig. 6). Near the leading edge and ahead of the initial disturbance, the pressures are not affected by interaction effects and hence probably check the theoretical values fairly closely. Behind the initial disturbance, the measured pressure coefficients are too high, with the discrepancy between the theoretical and experimental values being greatest on the lower or high-pressure and low-velocity side of the airfoil when it is at an angle of attack. Toward the trailing edge, the effect of a disturbance involving an expansion resulting from thinning of the tunnel boundary layer because of the favorable pressure gradient over the airfoil behind the shock tends to compensate somewhat the effect of the previous compressive disturbance, and the experimental pressure coefficients again are in better agreement with the theoretical values.

For models having larger leading-edge wedge angles and at lower free-stream Mach numbers, the rate at which the disturbance spreads probably will be much greater. This results from the fact that the Mach number behind the leading-edge shock will be relatively lower in these instances and the Mach or shock angles along which the disturbances propagate will be relatively greater. The magnitude of the pressure

disturbances also probably depends to a considerable extent on the ratio
of maximum model thickness to tunnel-wall boundary-layer thickness.
Where the model is relatively large compared to the boundary-layer thick-
ness the magnitude of the disturbances may be relatively small.

CONCLUSIONS

From the results of this investigation it may be concluded that,
when models are mounted from the tunnel wall in supersonic wind tunnels,
there is an interaction between the tunnel boundary layer and the flow
over the model which results in pressure distrubances over the model.
These disturbances spread farther out from the tunnel wall as the Mach
number on the model surface decreases either because of a lower free-
stream Mach number or an increase in angle of attack of the surfaces, and
may spread a considerable distance over the model at local Mach numbers
approaching unity or when the models are swept back. In general, strong
disturbances propagated from the boundary layer in the wing-tunnel-wall
juncture along a wave inclined at an angle slightly greater than the
Mach angle for the local stream. These results indicate the need for
very small airfoil-chord to wind-tunnel-span ratios or the use of boundary
layer removal devices in supersonic wind-tunnel testing where models are
mounted directly from the tunnel wall if the data are to be free from
interference effects. The problem also may be present in investigations
carried out on transonic bumps where the flow is supersonic either in
the free stream or in localized areas on the model. The same type of
disturbance may arise in the wing-fuselage juncture on supersonic air-
planes and may make it difficult to estimate the aerodynamic character-
istics of wing-fuselage combinations without extensive testing.

Langley Aeronautical Laboratory
        National Advisory Committee for Aeronautics
            Langley Field, Va.

REFERENCE

1. Ivey, H. Reese, Stickle, George W., and Schuettler, Alberta:
        Charts for Determining the Characteristics of Sharp-Nose Airfoils
        in Two-Dimensional Flow at Supersonic Speeds. NACA TN No. 1143,
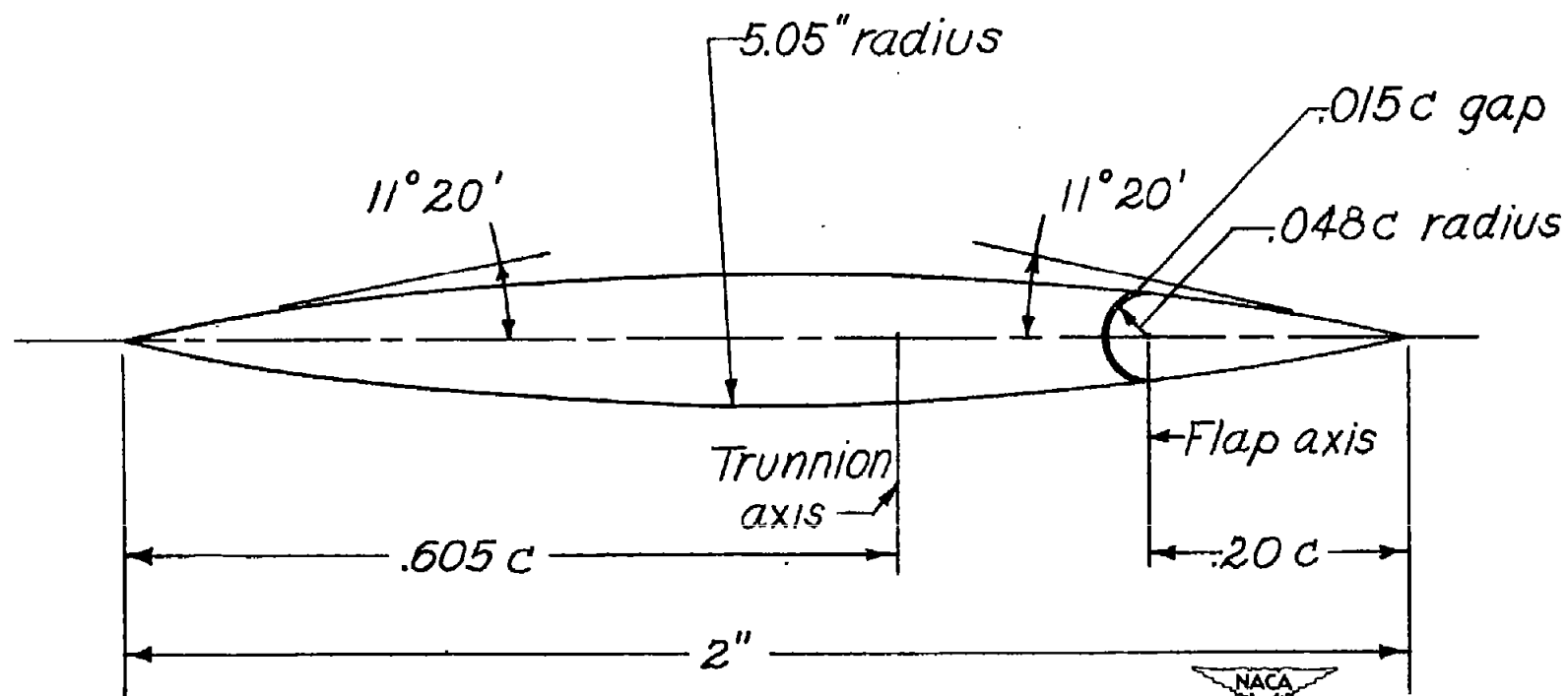   1947.

Figure 1.- Geometrical characteristics of the 10-percent-thick symmetrical circular-arc airfoil with 0.20c trailing-edge flap.
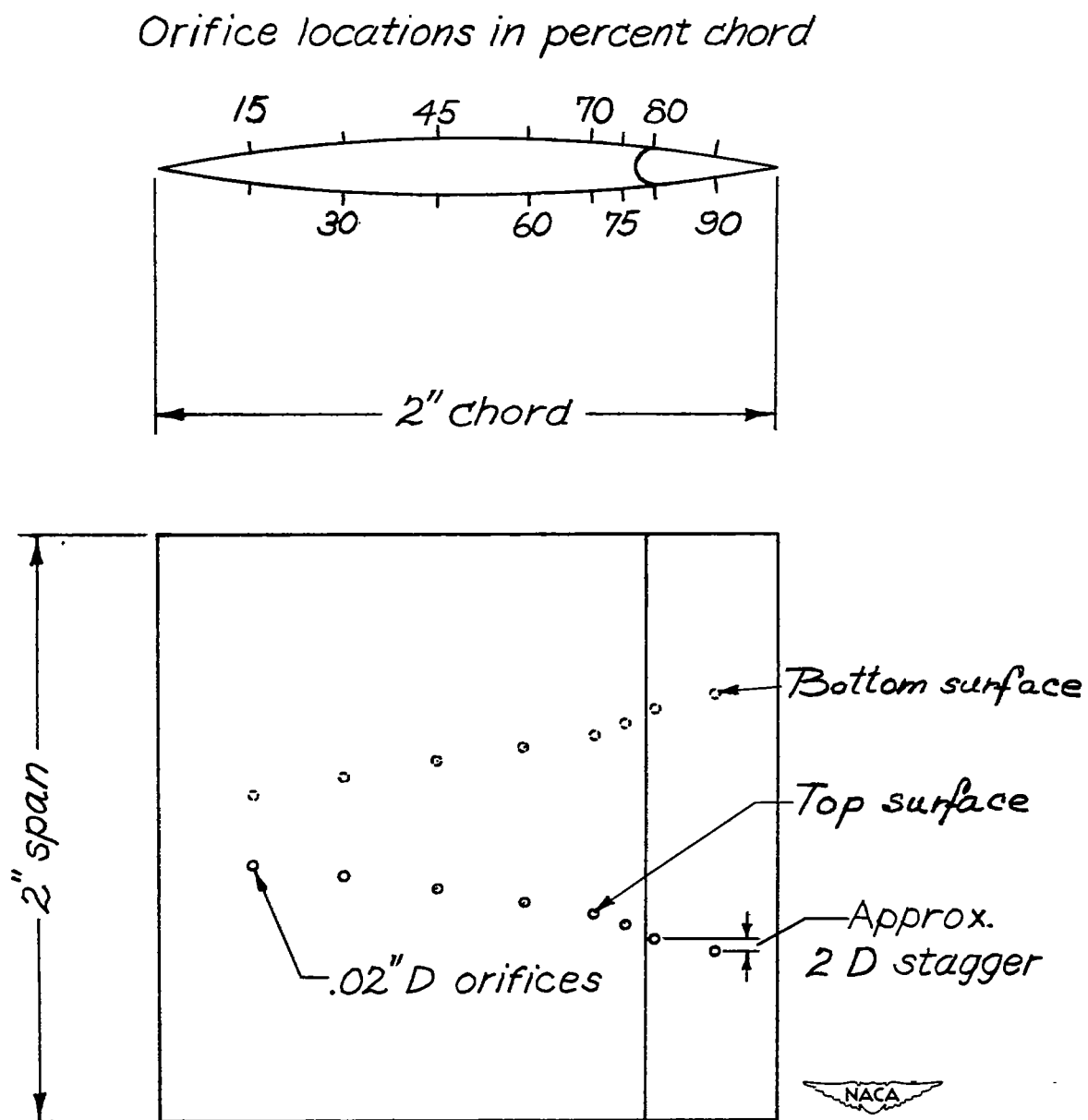
Orifice locations in percent chord

15   45   70 80

30   60 75 90

2" chord

2" span

Bottom surface

Top surface

.02" D orifices

Approx.
2 D stagger

NACA

Figure 2.- Sketch of airfoil with 0.20c trailing-edge flap showing orifice
locations.
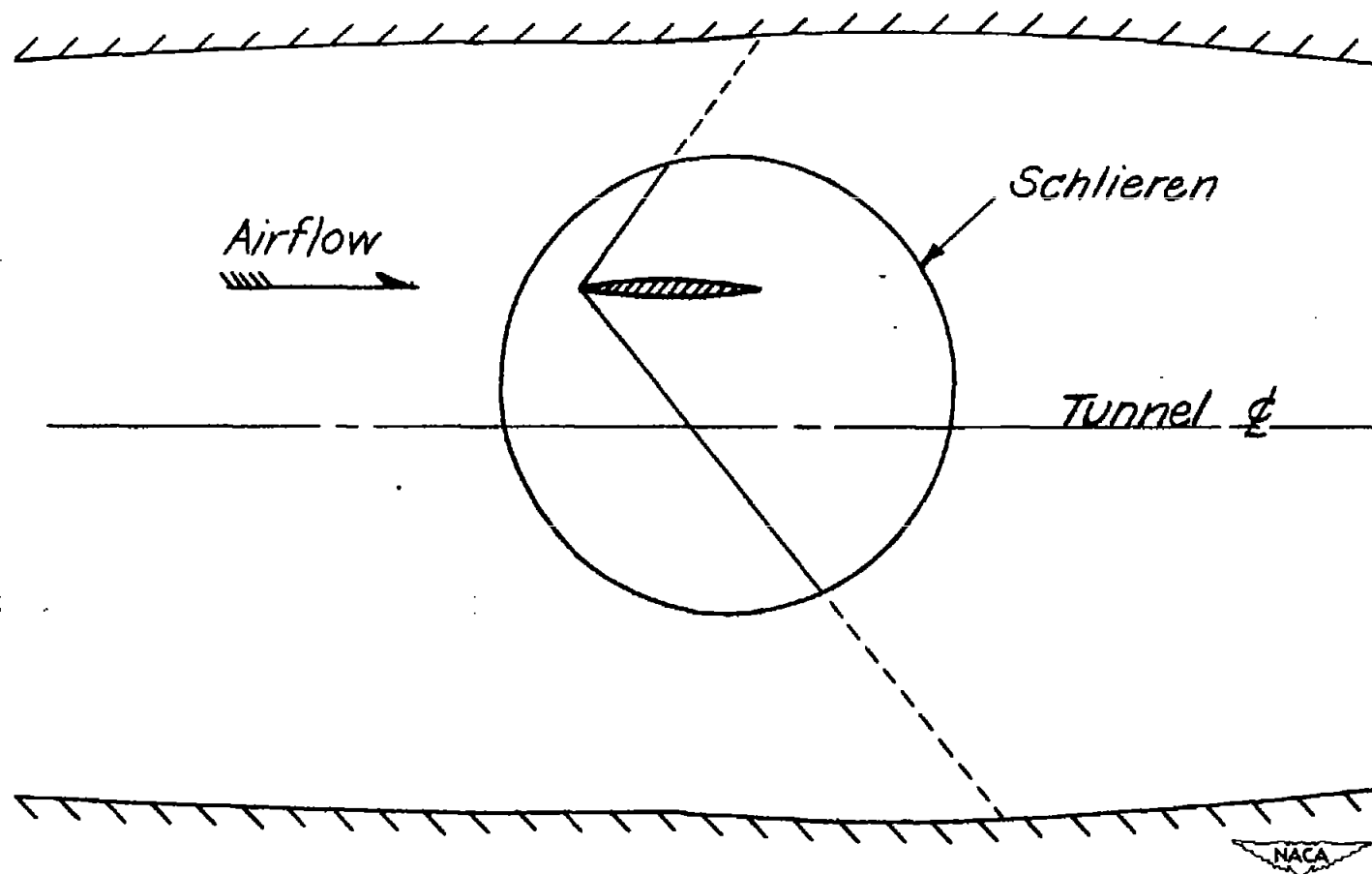
Figure 3.- Sketch of tunnel test section showing location of the model and schlieren in the 2-inch by 8-inch supersonic tunnel.
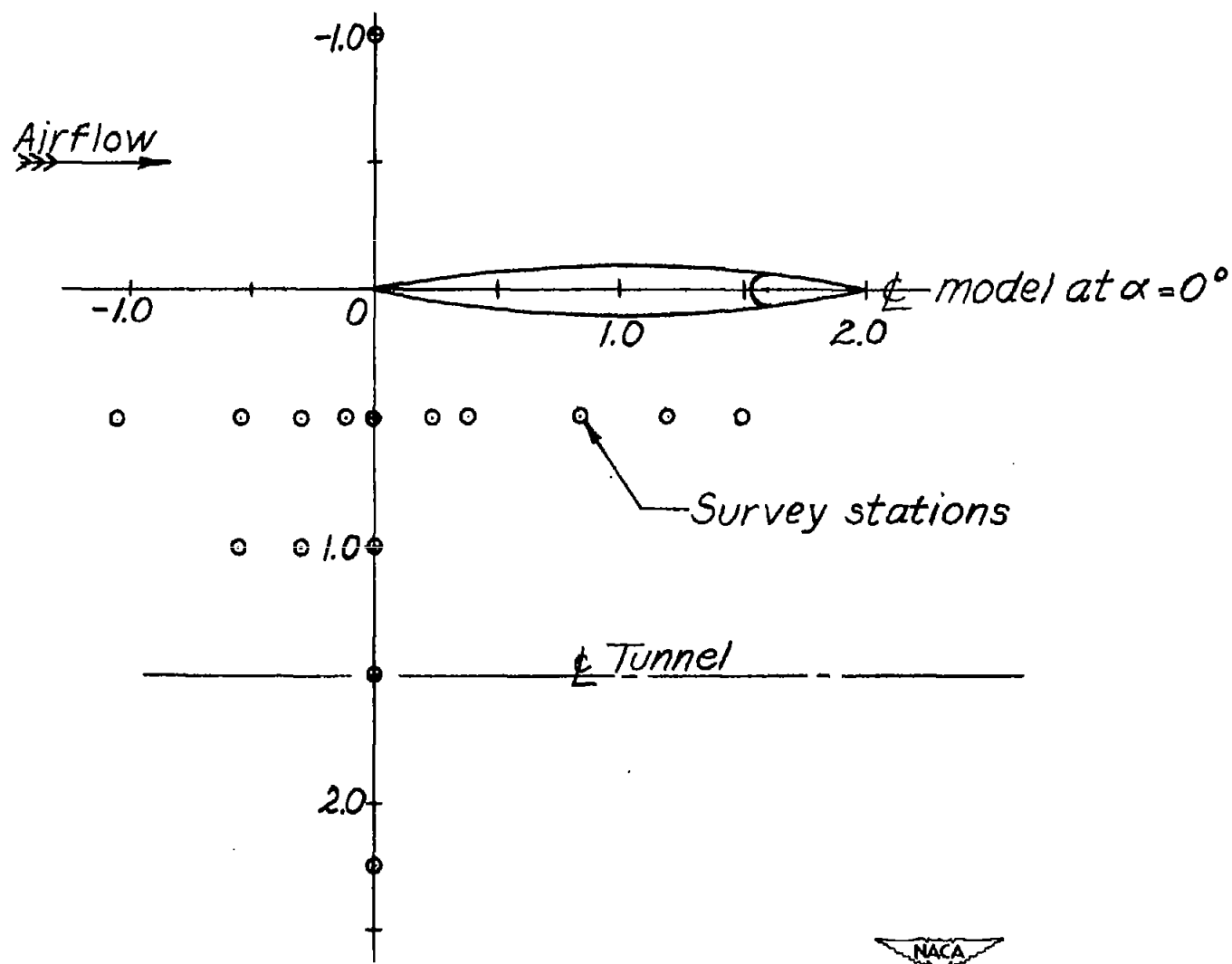
Figure 5.- Location of pressure-survey stations in the 2-inch by 8-inch supersonic tunnel. (Scale in inches.)
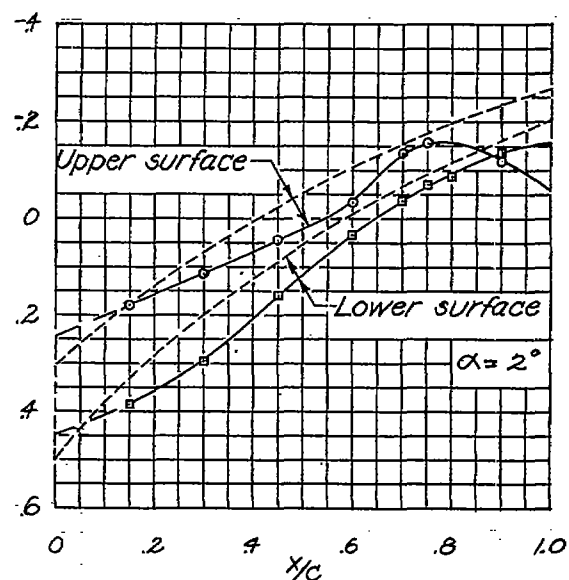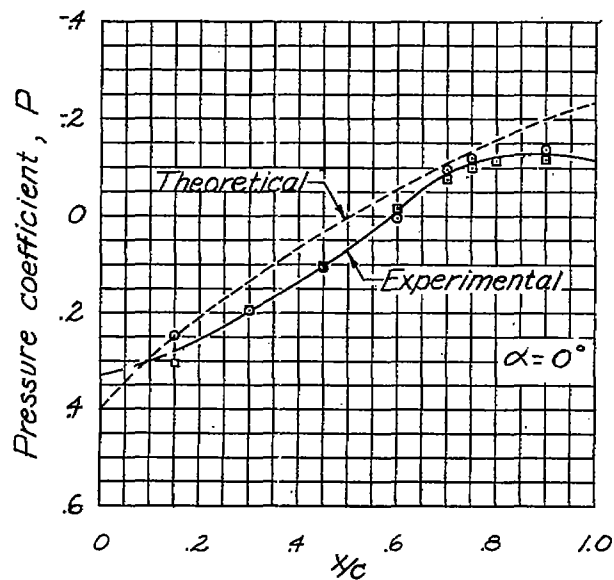
(a)   Airfoil with 0.20c flap.
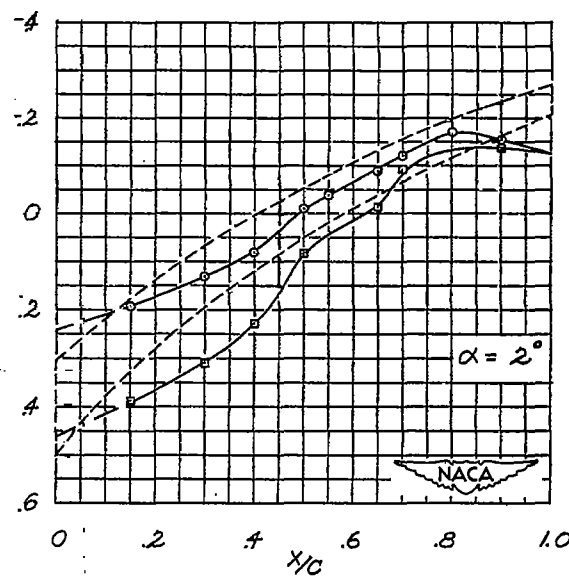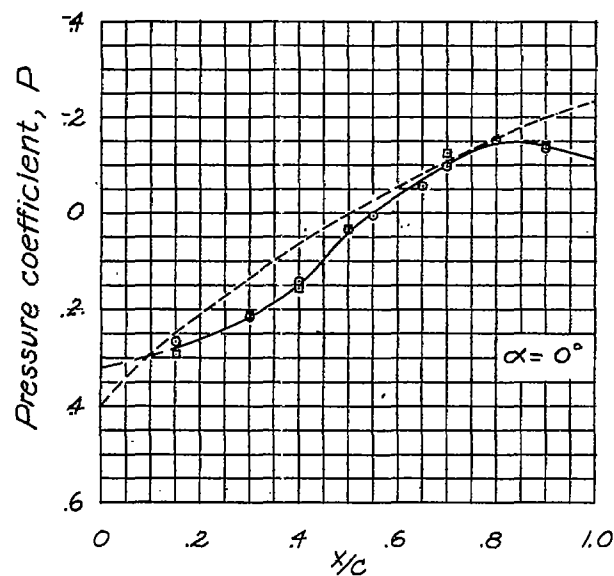
(b)   Airfoil with 0.40c flap.

Figure 6.-   Theoretical and experimental pressure distributions on two
10-percent-thick symmetrical circular-arc airfoils with trailing-edge
flaps.   M = 1.68;   δ = 0°.
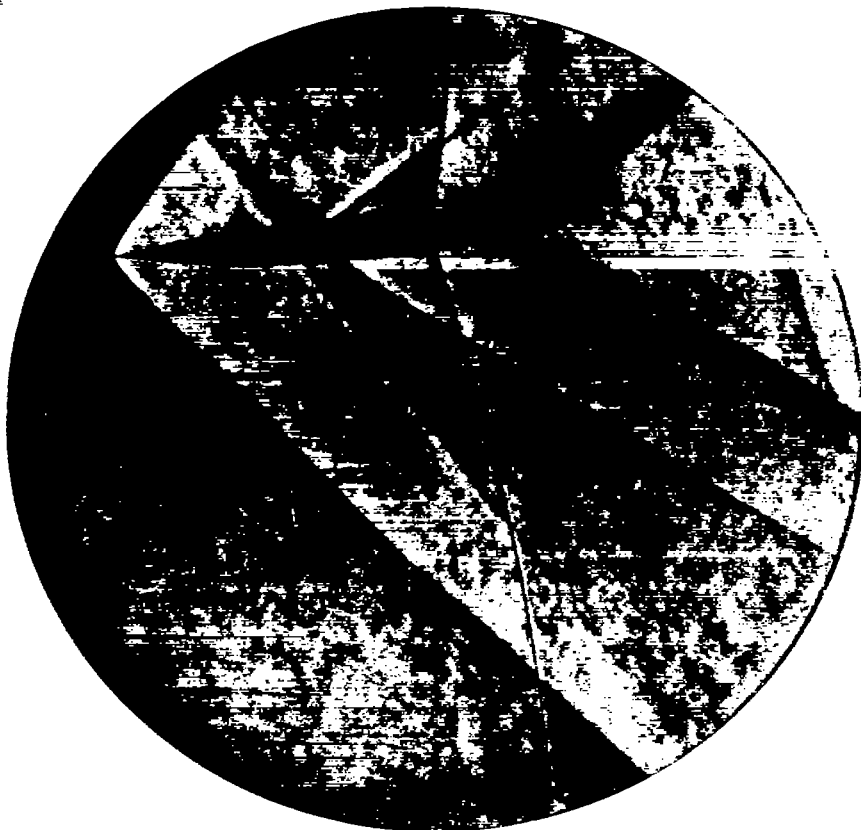
(a) 0.40c flap model.

Figure 7.- Schlieren photographs of 10-percent-thick symmetrical circular-
       arc airfoils in the 2- by 8-inch supersonic tunnel.   M = 1.68; $\alpha = 0^{\circ}$;
       $\delta = 0^{\circ}$.
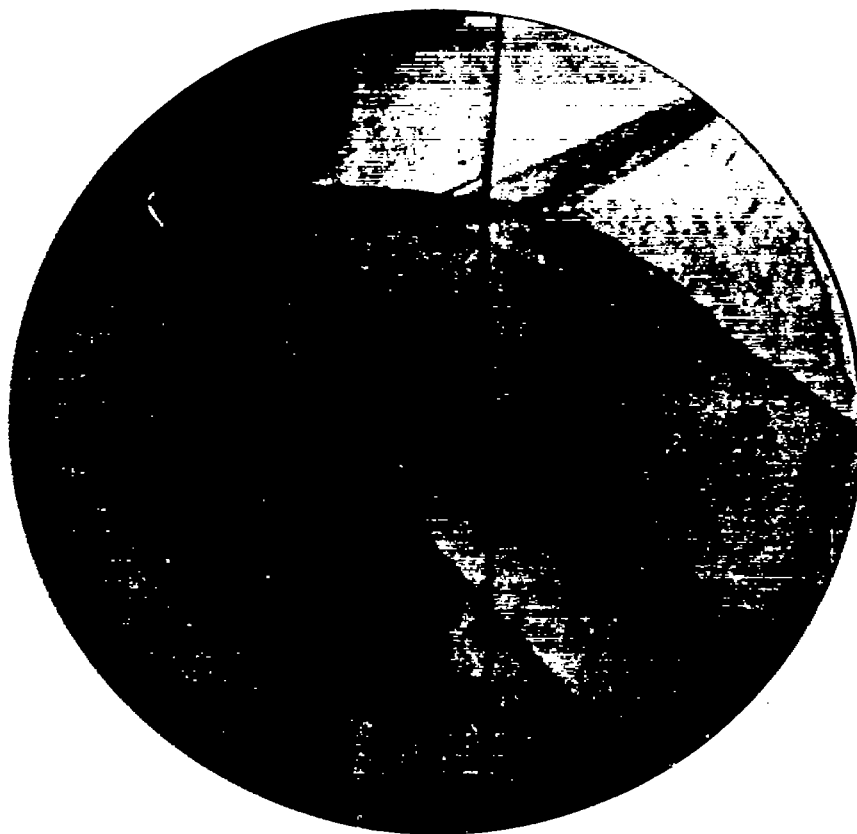
(b)   0.20c flap model.

Figure 7.- Concluded.
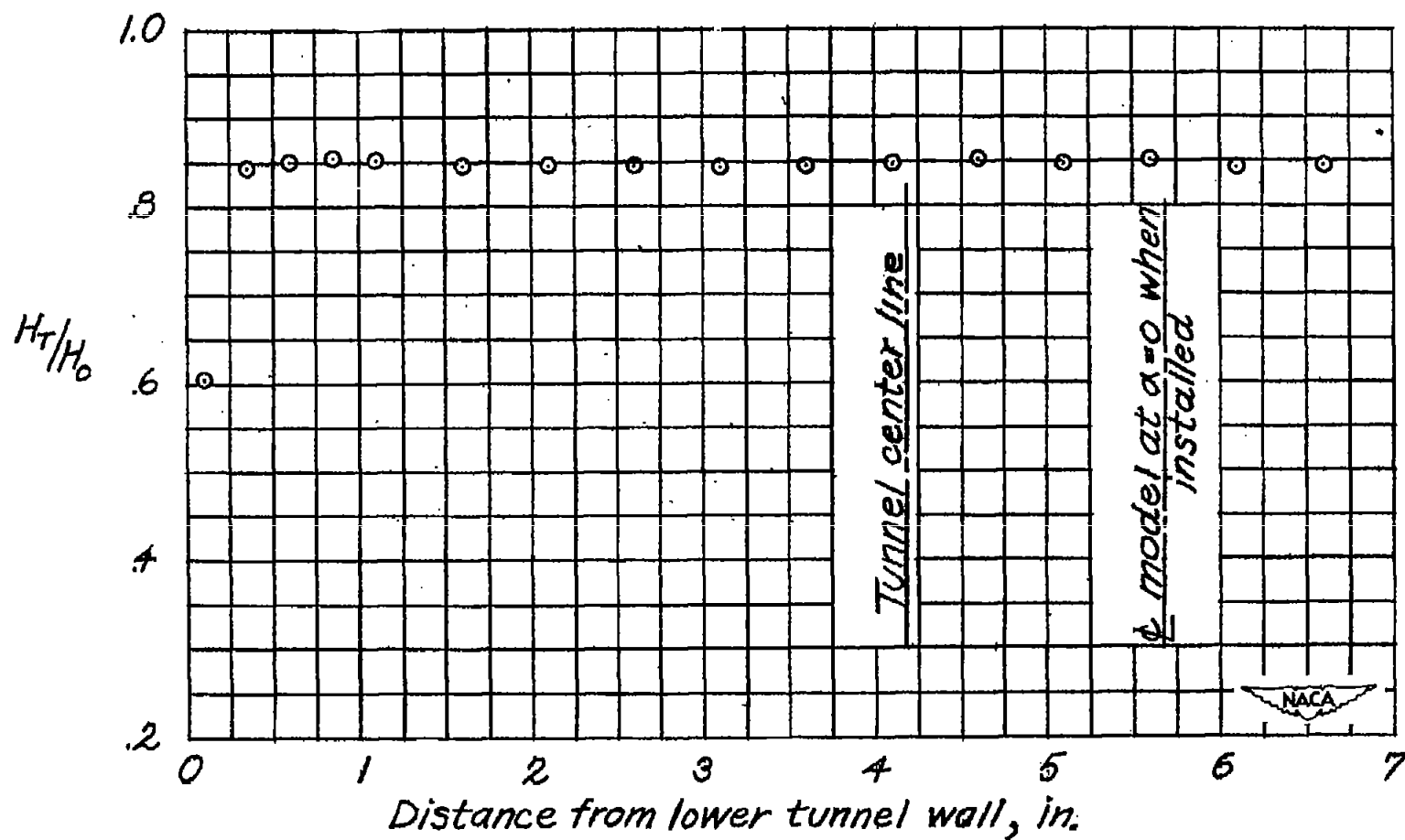
Figure 8.- Variation of the ratio of uncorrected measured total pressure to measured stagnation pressure across the test section in the 8-inch direction of the 2-inch by 8-inch supersonic tunnel. Jet empty.
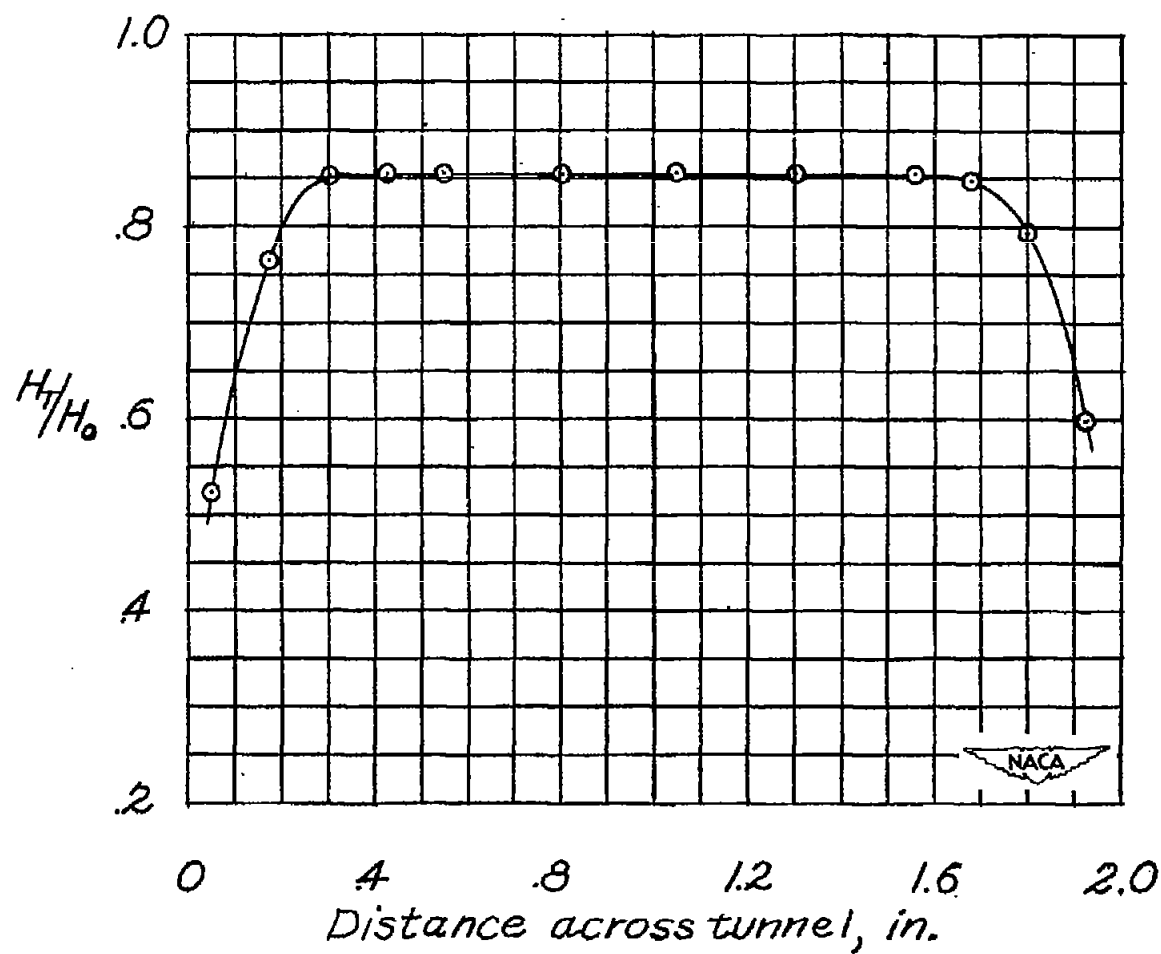
Figure 9.- Typical spanwise variation in the ratio of uncorrected measured total pressure to measured stagnation pressure in the 2-inch by 8-inch supersonic tunnel. Jet empty.
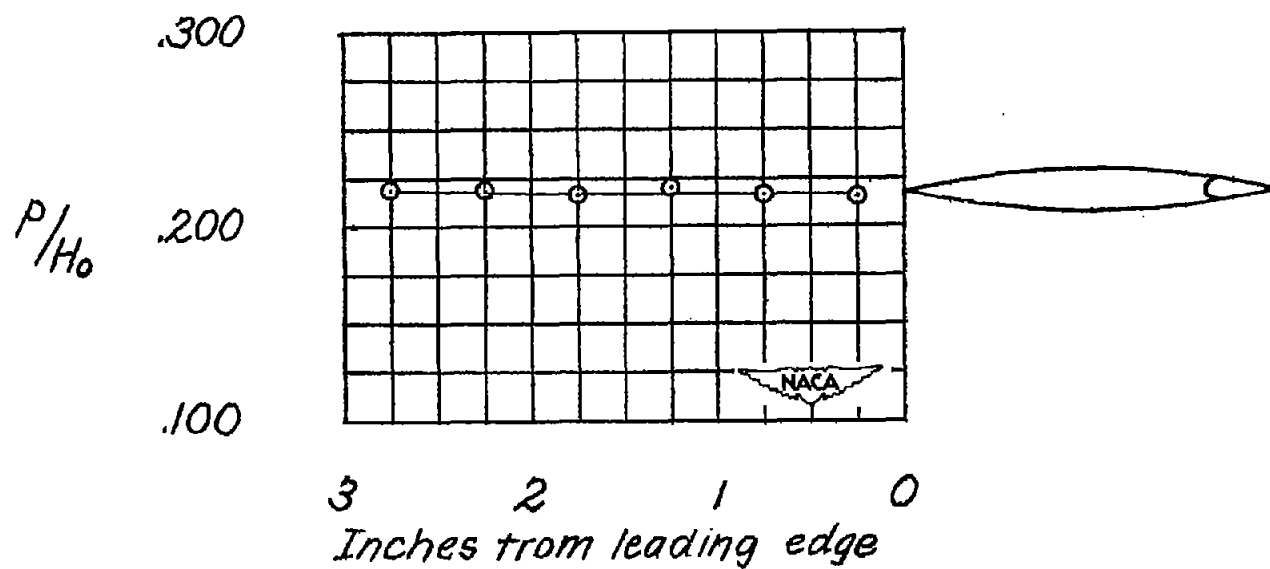
Figure 10.- Variation of the ratio of measured wall static pressure to measured stagnation pressure along the tunnel wall at the model center line in the 2-inch by 8-inch supersonic tunnel.
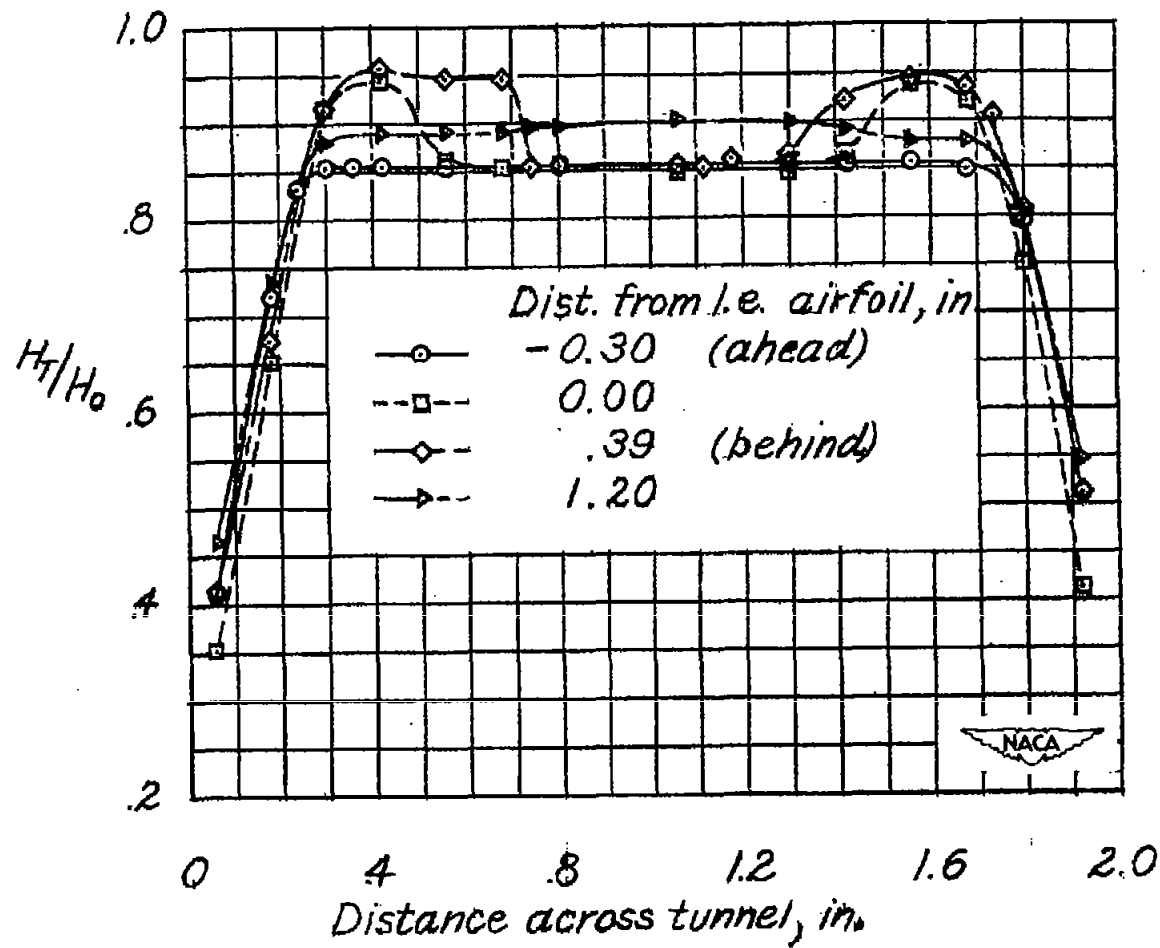
Figure 11.- Typical spanwise variation in the ratio H_T/H_0 in the 2-inch by 8-inch supersonic tunnel at various distances from leading edge of a 10-percent-thick symmetrical circular-arc airfoil. Surveys in plane parallel to and 1/2 inch below center line of model; $\alpha = 0^\circ$.
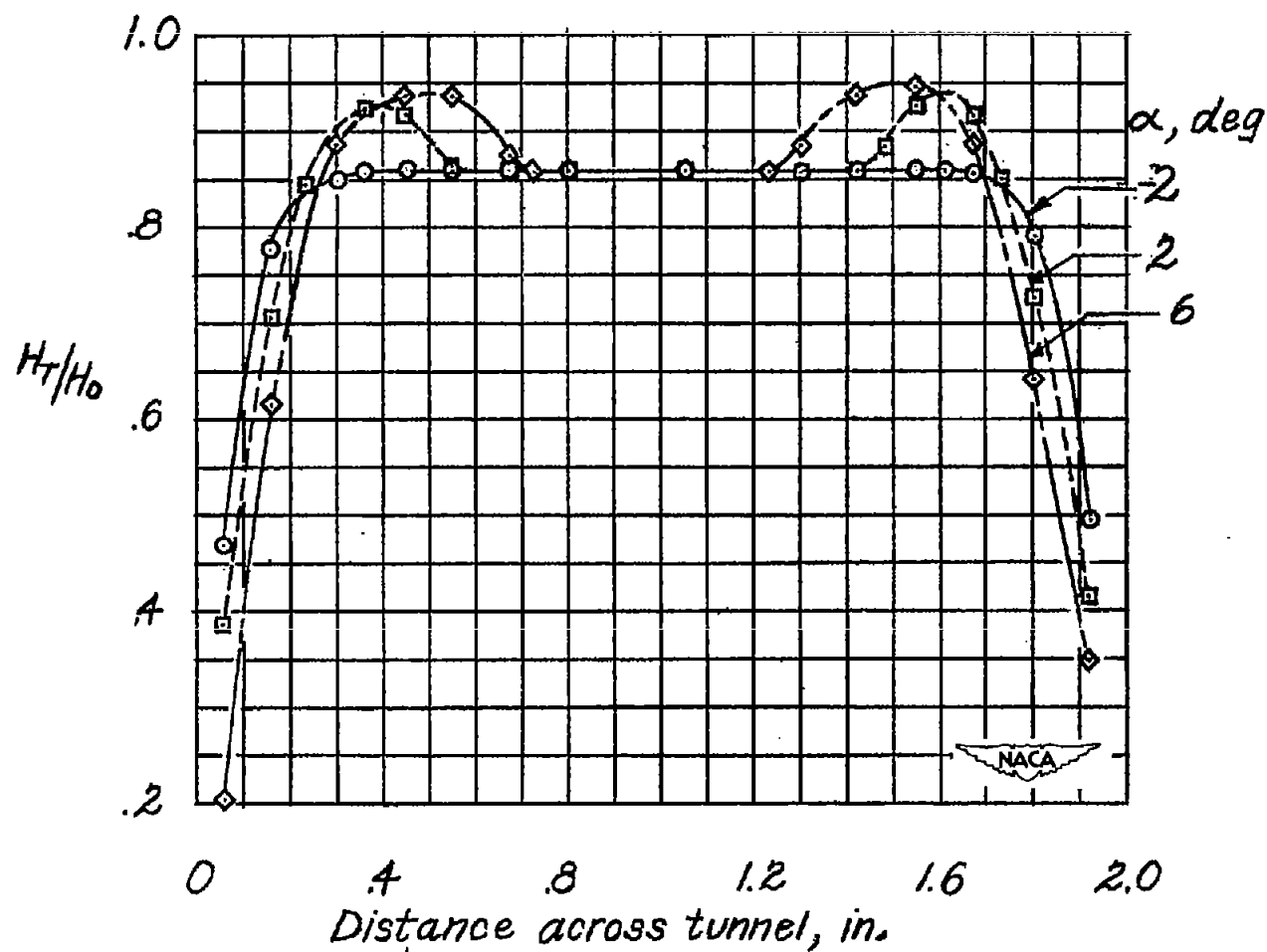
Figure 12.- Effect of angle of attack on spanwise variation in the ratio H_T/H_o in the 2-inch by 8-inch supersonic tunnel with a 10-percent-thick symmetrical circular-arc airfoil installed. Surveys in plane of leading edge and 1 inch below center line of model.
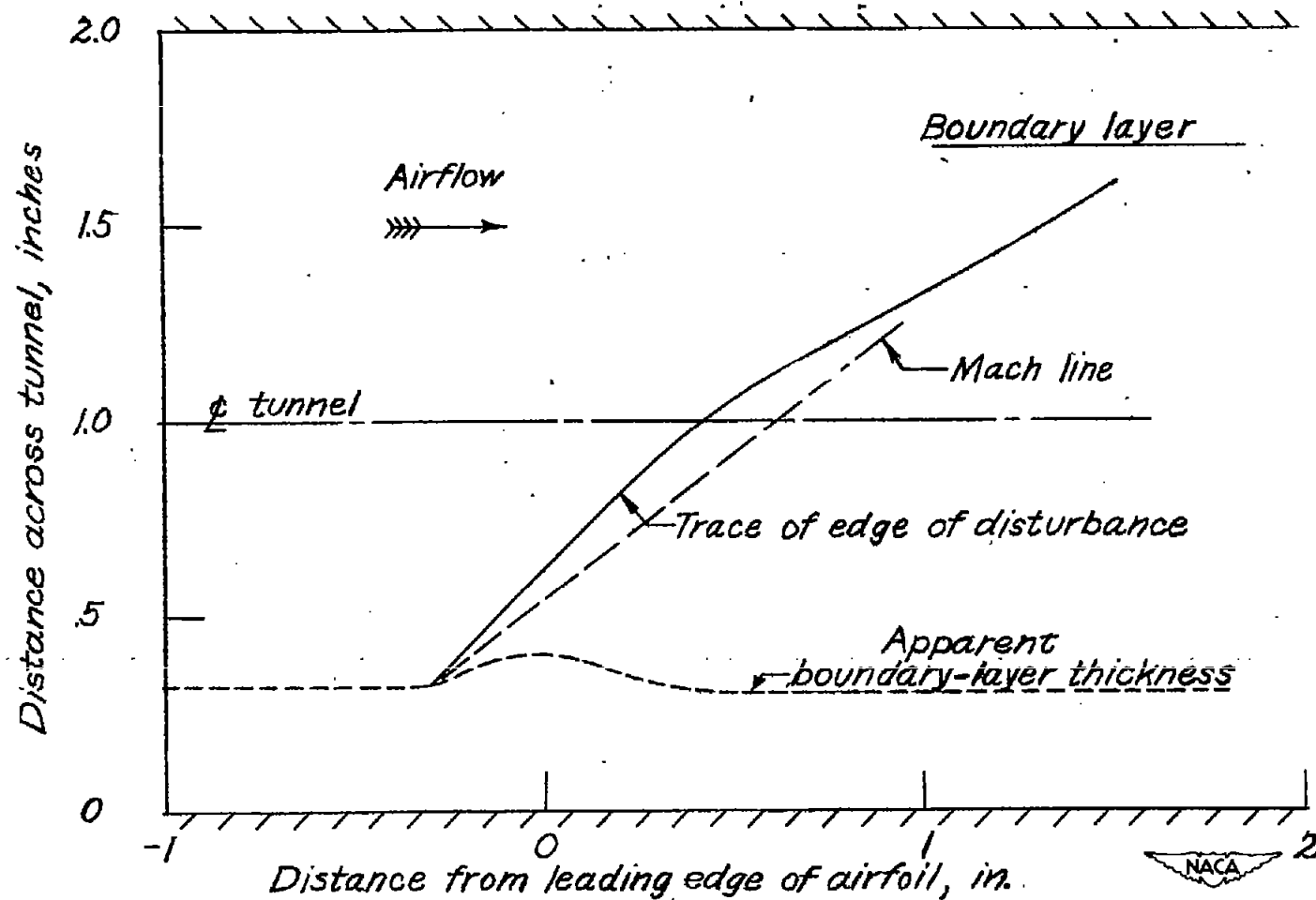
Figure 13.- Average variation of boundary-layer thickness and trace of edge of disturbance along test nozzle with model installed. Half inch below center line of airfoil; $\alpha = 0^\circ$ and 2°; 2-inch by 8-inch supersonic tunnel.
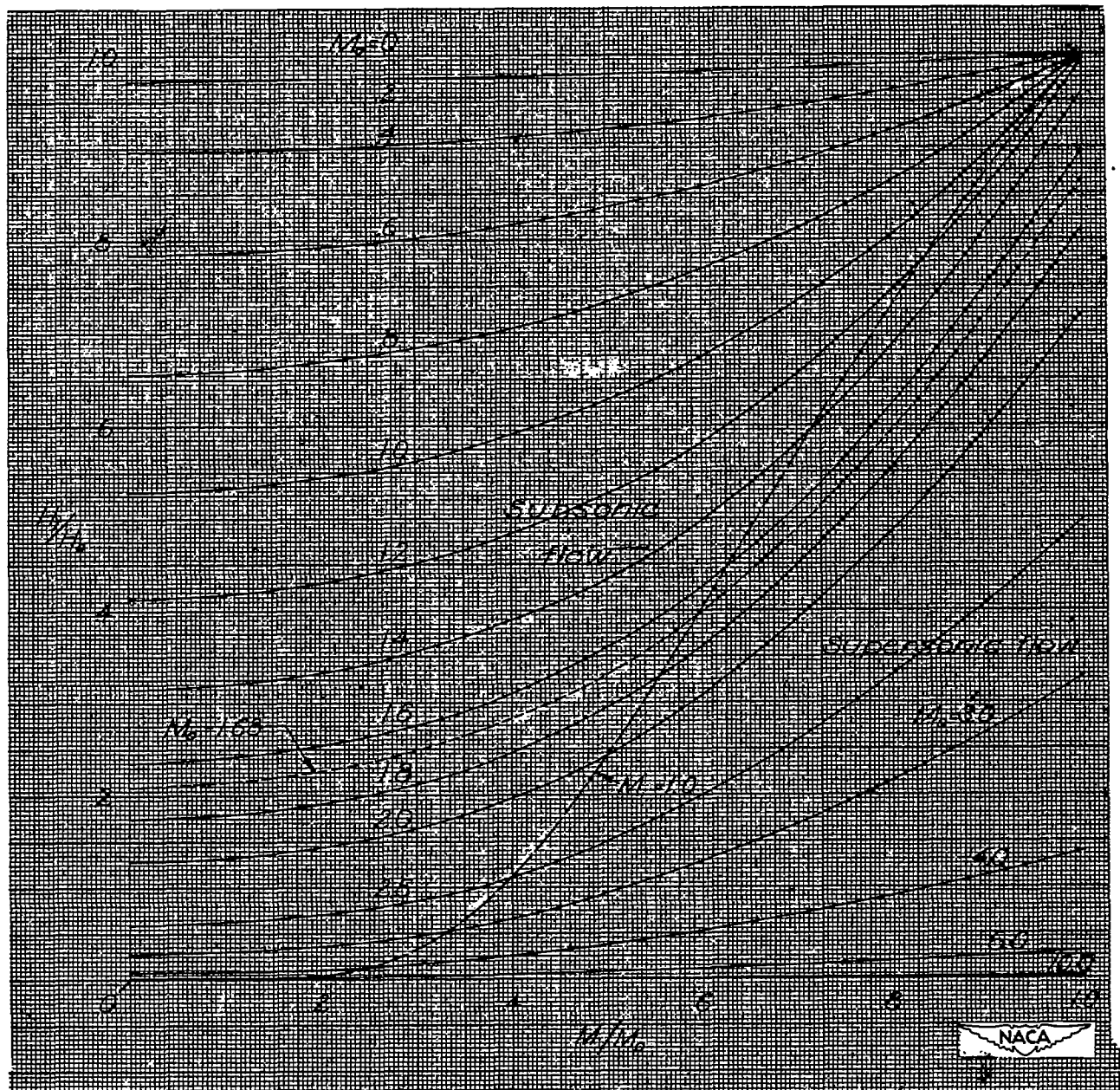
Figure 14.- Theoretical variation of H_T/H_o with M/M_o in a boundary layer with static pressure constant and equal to free-stream static pressure.